MOBY

MOdeling **B**inar**Y** Systems That End in Stellar Mergers and Give Rise to Gravitational Waves

Jelena Petrović
Astronomska Opservatorija Beograd

Фонд за науку
Републике Србије

MOBY project

The newest observations of gravitational waves, by the Virgo and LIGO telescopes, indicate that the observed radiation originates in mergers of black holes with masses up to 100 $M_\odot$.

Within the MOBY project, the progenitor evolution of such gravitational wave sources, related to the most massive double black holes is investigated.

The evolutionary models of rotating close (Case A) massive binary systems are calculated with the MESA (Modules for Experiments in Stellar Astrophysics) numerical code.

The goal of the MOBY project is to produce an extensive grid of detailed evolutionary models of rotating massive binary systems with the initial masses between 100 $M_\odot$ and 250 $M_{\odot,}$ in order to reproduce double black hole systems with masses above 50 $M_\odot$ and constrain the initial and other physical parameters of possible progenitors of gravitational wave sources.

MOBY team

dr. Jelena Petrović,PI
Full Research
Professor, AOB

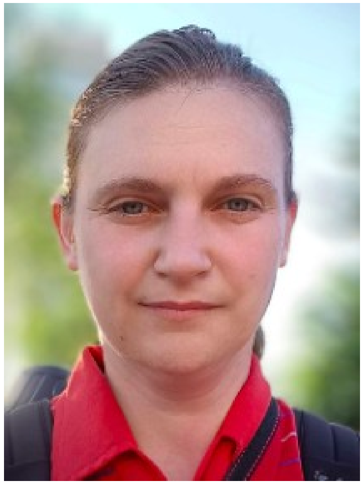

dr. Monika Jurković,
Assistant Professor,
AOB

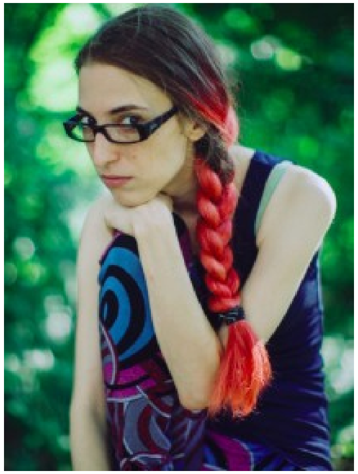

dr. Ana Mitrašinović,
Assistant Professor,
AOB

Prof.dr. Bojan Arbutina
Full Professor, MATF

dr. Gojko Đurašević
Full Research
Professor, AOB

+ PhD student – Natalija Mladenović

First GW observations

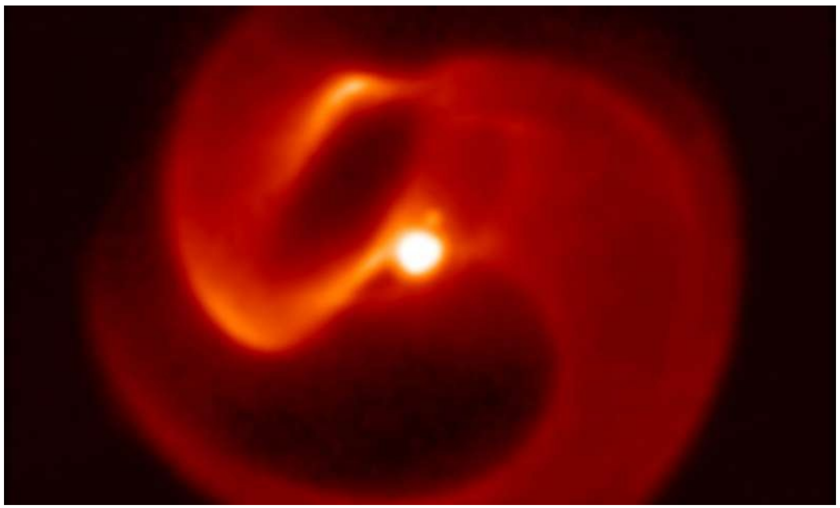

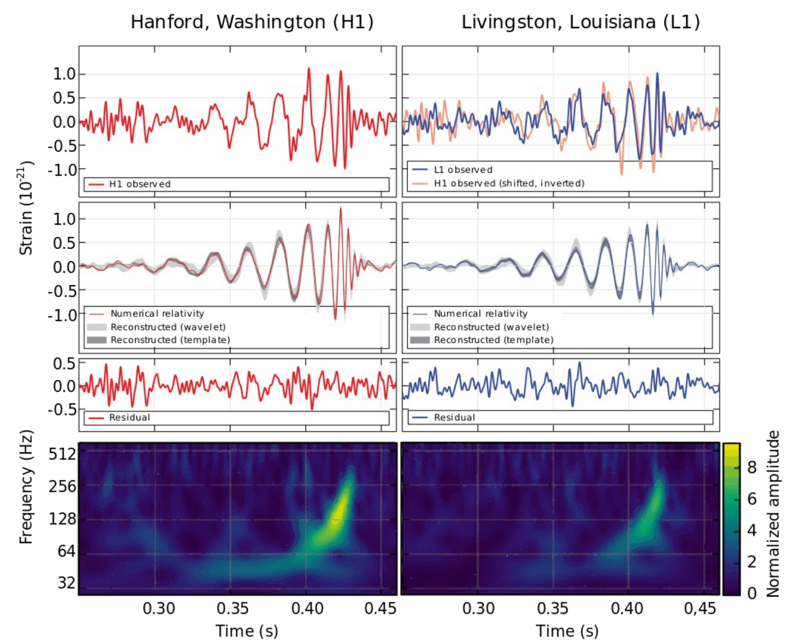

14.09.2015 - binary system of two BH $29M_\odot + 36M_\odot$ – GW150914 (LIGO)

16.10.2017 binary system of two NS about $2M_\odot$ each GW170817 (LIGO and VIRGO)

LIGO & Virgo observations (https://gwosc.org/eventapi/html/allevents/)

List contains 93 events.

Focus

Display all | Display

Name	Version	Release	GPS	Mass 1 ($M_\odot$)	Mass 2 ($M_\odot$)	Network SNR	Distance (Mpc)	χ_{eff}	Total Mass ($M_\odot$)
GW190426_190642	v1	GWTC-2.1-confident	1240340820.6	$105.5^{+45.3}_{-24.1}$	$76.0^{+26.2}_{-36.5}$	$8.7^{+0.4}_{-0.6}$	4580^{+3400}_{-2280}	$0.23^{+0.42}_{-0.41}$	$182.3^{+40.2}_{-35.7}$
GW190521	v4	GWTC-2.1-confident	1242442967.4	$98.4^{+33.6}_{-21.7}$	$57.2^{+27.1}_{-30.1}$	$14.3^{+0.5}_{-0.4}$	3310^{+2790}_{-1800}	$-0.14^{+0.50}_{-0.45}$	$153.1^{+42.2}_{-16.2}$
GW200220_061928	v1	GWTC-3-confident	1266214786.7	87^{+40}_{-23}	61^{+26}_{-25}	$7.2^{+0.4}_{-0.7}$	6000^{+4800}_{-3100}	$0.06^{+0.40}_{-0.38}$	148^{+55}_{-33}
GW190403_051519	v1	GWTC-2.1-confident	1238303737.2	$85.0^{+27.8}_{-33.0}$	$20.0^{+26.3}_{-8.4}$	$7.6^{+0.6}_{-1.1}$	8280^{+6720}_{-4290}	$0.68^{+0.16}_{-0.43}$	$106.6^{+26.7}_{-23.6}$
GW190706_222641	v2	GWTC-2.1-confident	1246487219.3	$74.0^{+20.1}_{-16.9}$	$39.4^{+18.4}_{-15.4}$	$13.4^{+0.2}_{-0.4}$	3630^{+2600}_{-2000}	$0.28^{+0.25}_{-0.31}$	$112.6^{+27.4}_{-16.8}$
GW190602_175927	v2	GWTC-2.1-confident	1243533585.0	$71.8^{+18.1}_{-14.6}$	$44.8^{+15.5}_{-19.6}$	$13.2^{+0.2}_{-0.3}$	2840^{+1930}_{-1280}	$0.12^{+0.25}_{-0.28}$	$115.6^{+19.2}_{-14.8}$
GW190929_012149	v2	GWTC-2.1-confident	1253755327.4	$66.3^{+21.6}_{-16.6}$	$26.8^{+14.7}_{-10.6}$	$9.7^{+0.4}_{-0.6}$	3130^{+2510}_{-1370}	$-0.03^{+0.23}_{-0.28}$	$93.3^{+23.3}_{-15.0}$
GW190519_153544	v2	GWTC-2.1-confident	1242315362.3	$65.1^{+10.8}_{-11.0}$	$40.8^{+11.5}_{-12.7}$	$15.9^{+0.2}_{-0.3}$	2600^{+1720}_{-960}	$0.33^{+0.20}_{-0.24}$	$105.6^{+14.4}_{-13.9}$
GW191109_010717	v1	GWTC-3-confident	1257296855.2	65^{+11}_{-11}	47^{+15}_{-13}	$17.3^{+0.5}_{-0.5}$	1290^{+1130}_{-650}	$-0.29^{+0.42}_{-0.31}$	112^{+20}_{-16}
GW200308_173609	v1	GWTC-3-confident	1267724187.7	60^{+166}_{-29}	24^{+36}_{-13}	$4.7^{+2.5}_{-2.9}$	7100^{+13900}_{-4400}	$0.16^{+0.58}_{-0.49}$	$92.0^{+169.0}_{-48.0}$
GW190620_030421	v2	GWTC-2.1-confident	1245035079.3	$58.0^{+19.2}_{-13.3}$	$35.0^{+13.1}_{-14.5}$	$12.1^{+0.3}_{-0.4}$	2910^{+1710}_{-1320}	$0.34^{+0.22}_{-0.29}$	$92.7^{+18.5}_{-13.2}$
GW190701_203306	v2	GWTC-2.1-confident	1246048404.5	$54.1^{+12.6}_{-8.0}$	$40.5^{+8.7}_{-12.1}$	$11.2^{+0.2}_{-0.4}$	2090^{+770}_{-740}	$-0.08^{+0.23}_{-0.31}$	$94.3^{+12.0}_{-9.5}$
GW191127_050227	v1	GWTC-3-confident	1258866165.5	53^{+47}_{-20}	24^{+17}_{-14}	$9.2^{+0.7}_{-0.6}$	3400^{+3100}_{-1900}	$0.18^{+0.34}_{-0.36}$	80^{+39}_{-22}
GW190413_134308	v2	GWTC-2.1-confident	1239198206.7	$51.3^{+16.6}_{-12.6}$	$30.4^{+11.7}_{-12.7}$	$10.6^{+0.4}_{-0.5}$	3800^{+2480}_{-1830}	$-0.01^{+0.28}_{-0.38}$	$81.3^{+16.8}_{-11.8}$
GW200208_222617	v1	GWTC-3-confident	1265235995.9	51^{+103}_{-30}	$12.3^{+9.2}_{-5.5}$	$7.4^{+1.4}_{-1.2}$	4100^{+4400}_{-2000}	$0.45^{+0.42}_{-0.46}$	63^{+100}_{-26}

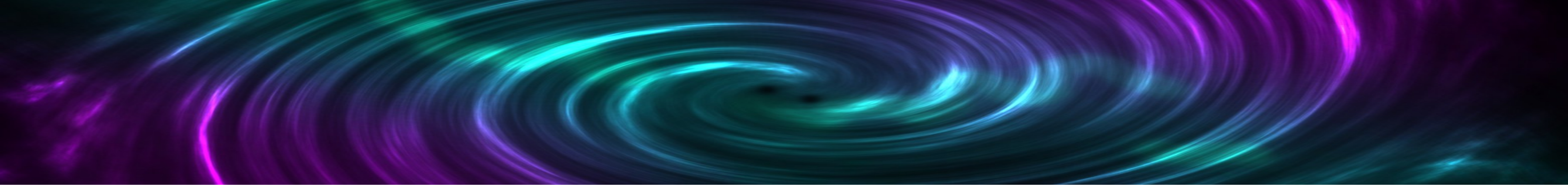

Massive binary systems

The evolution of a star in a binary system differs significantly from that of an isolated one with the same mass and chemical composition and are related to:

- Wolf-Rayet stars
- X ray emission
- Ib/c supernovae explosions
- Gamma ray bursts / Collapsars
- **Gravitational waves**

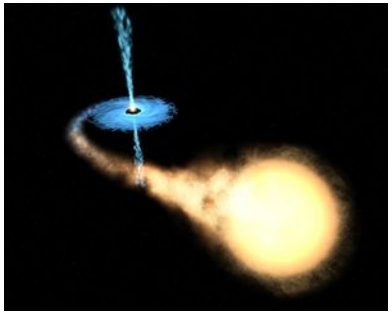

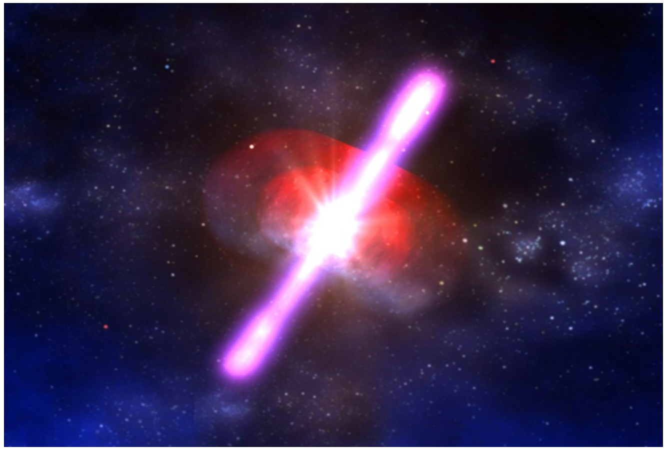

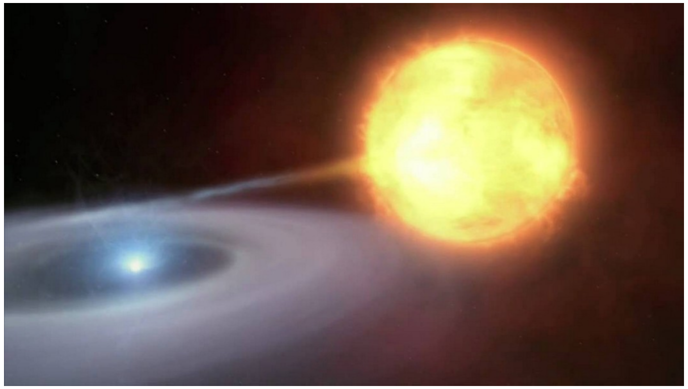

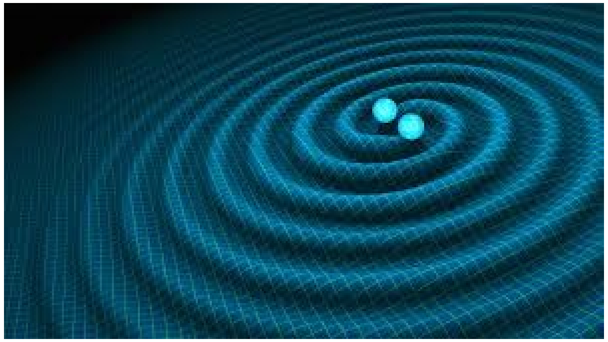

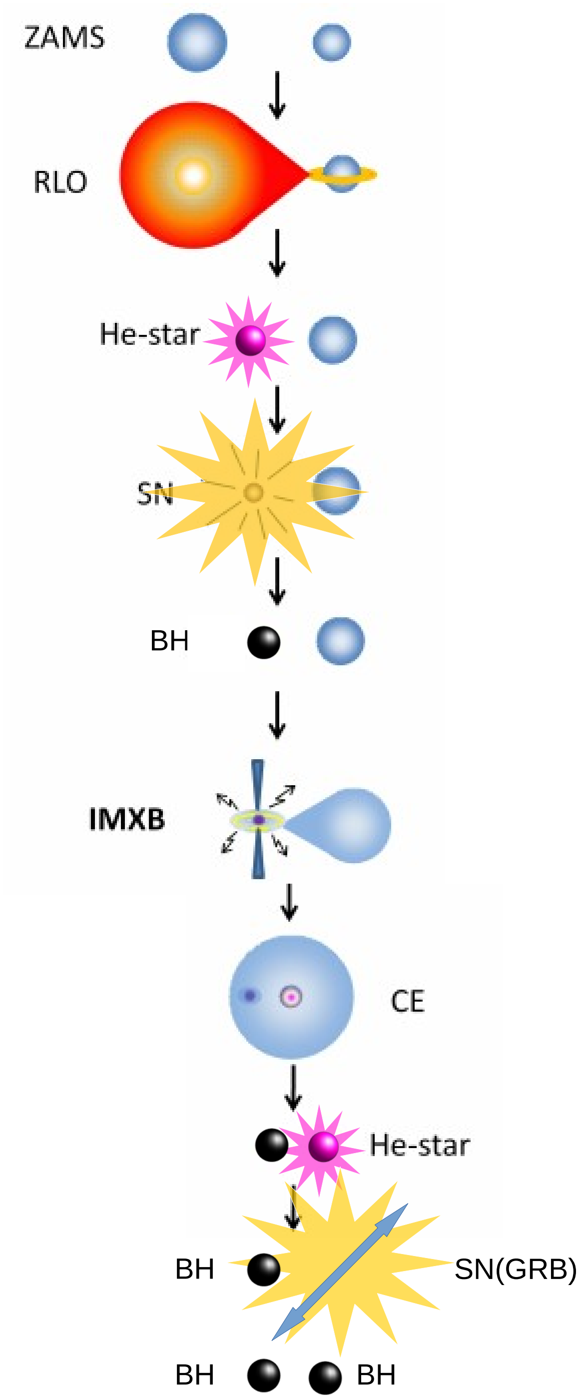

Evolution of massive binary systems

Depending on an initial period, the primary star fills its Roche lobe during the hydrogen core burning, hydrogen shell burning or helium shell burning phase and mass transfer to the secondary starts: **Case A**, **Case B** or **Case C** respectively.

The primary becomes **Wolf Rayet** (He) star that eventually explodes as a supernova Ib/c type and leaves a black hole as a remnant.

If the secondary fills its Roche lobe, mass transfer to the compact object starts accompanied by **x-ray emission.**

Common Envelope can happen during any mass transfer phase and lead to a shortening of a period or a merger.

If the secondary star is rotating fast in moment of supernova explosion, a **collapsar** is formed: fast spinning black hole with accretion disk and jets – **gamma-ray burst** can be observed.

Double black hole (Double compact object DCO) as a final evolutionary stage of a massive binary system.

Merger of compact objects can be a source of **Gravitational Waves.**

Rotation in binary systems & accretion efficiency

Components in binary systems **synchronize** its rotation with the orbital period due to tidal processes, so rotation velocities of binary stars can be very different from rotational velocities of single star with the same mass (Heger & Langer 2000, Meynet & Maeder 2000).

During mass transfer, mass and angular momentum are transferred to the accretor, this influences rotation velocity as well and can increase it to a so-called **critical rotation**.

When star reaches its critical rotation, it undergoes **extremely high mass loss** due to a stellar wind (Langer 1997, 1998).

Estimates of the angular momentum gain of the accreting star in mass transferring binaries show that critical rotation may be reached quickly (Langer et al. 2000; Yoon & Langer 2004) and the effective mass accretion rate can be significantly decreased due to the spin-up of the mass receiving star (Wellstein 2001; Langer et al. 2003, 2004; Petrovic et al. 2005a).

Fast rotating massive star in can evolve into a collapsar: fast rotating BH connected with Gamma Ray Bursts (first models: Petrovic et al. 2005b; Heger et al. 2005; Woosley 2004)

Massive binary evolution example – HR diagram

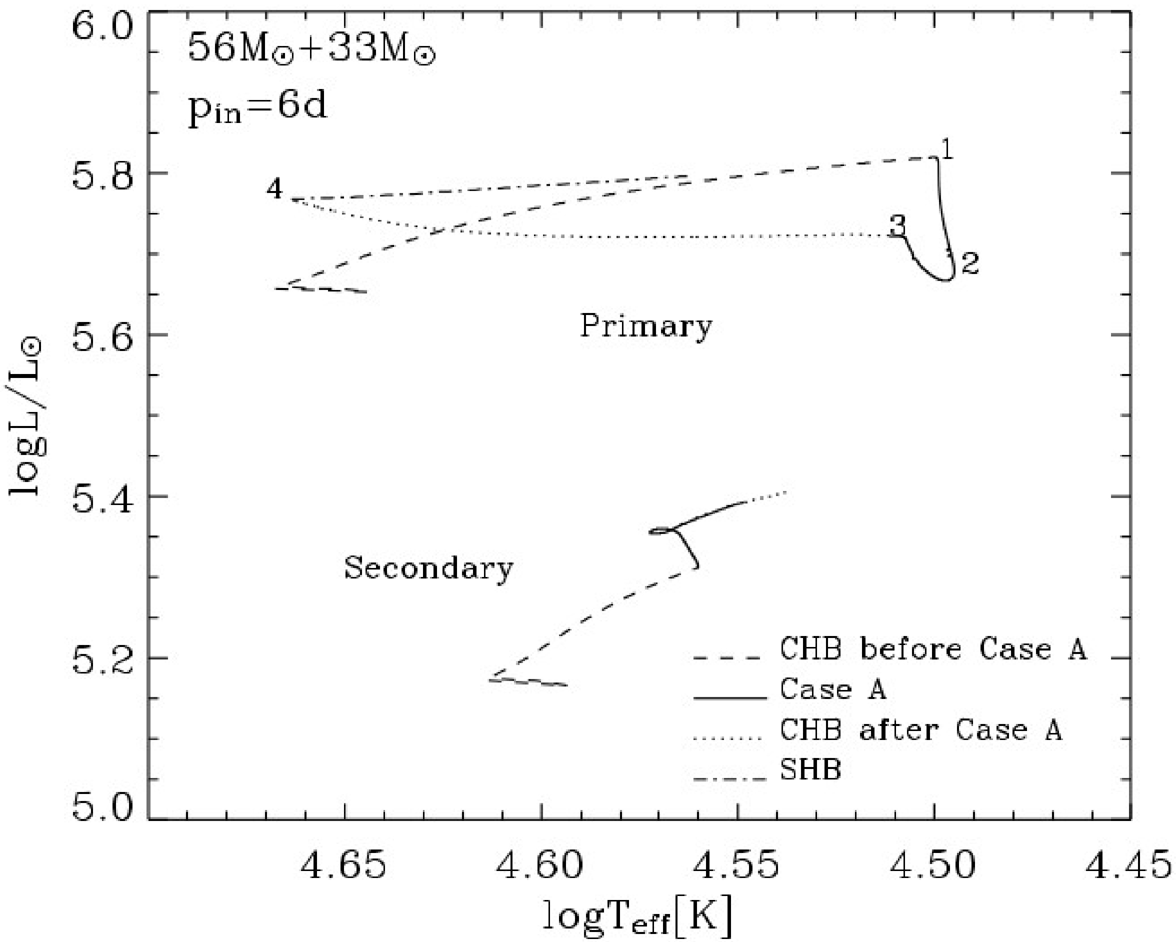

Rotating model 56 $M_\odot$ + 33 $M_\odot$
Initial period 6 days

Fig. 3. HR diagram of the initial system $M_{1,in} = 56\,M_\odot$, $M_{2,in} = 33\,M_\odot$, $p_{in} = 6$ days. Both stars are core hydrogen burning (dashed line) until Case A mass transfer starts (solid line). The primary is losing mass and its luminosity and effective temperature decrease. At the same time the secondary is accreting matter and expanding, becoming more luminous and cooler. After Case A mass transfer is finished, the primary is losing mass by stellar wind and contracting at the end of core hydrogen burning (dotted line). After this the primary starts with shell hydrogen burning and expands (dash-dotted line).

Petrovic, Langer, van der Hucht, 2005

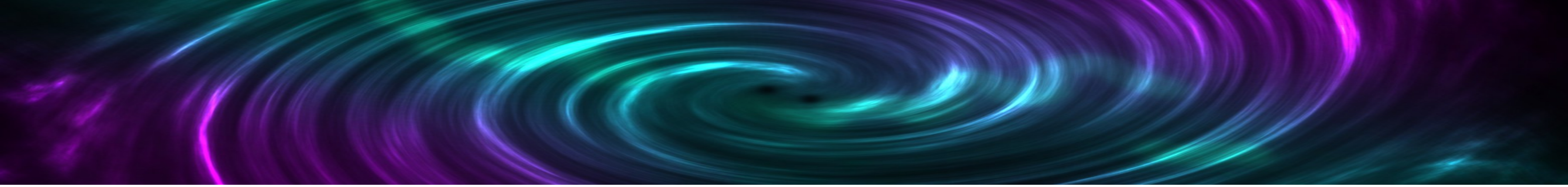

Massive binary evolution example – rotation & accretion

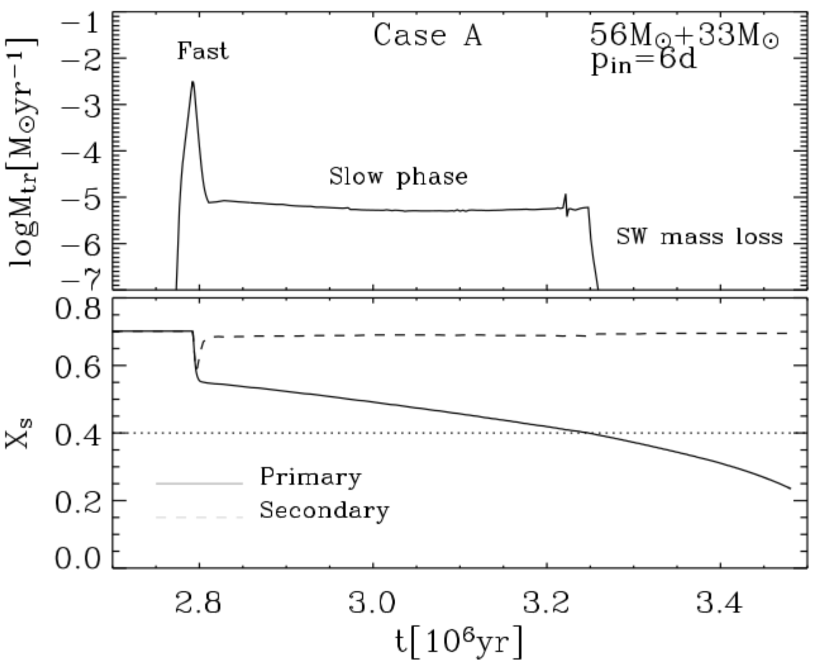

Fig. 6. *Upper plot*: mass transfer rate during Case A mass transfer in the binary system with $M_{1,\mathrm{in}} = 56\,M_\odot$, $M_{2,\mathrm{in}} = 33\,M_\odot$, $p_\mathrm{in} = 6$ days. *Lower plot*: the hydrogen surface abundance of the primary (solid line) is decreasing during mass transfer and further due to stellar wind mass loss. The secondary (dashed line) recovered its original surface hydrogen abundance through thermohaline mixing. The primary starts losing mass with WR stellar wind mass loss when its hydrogen surface abundance falls beneath $X_\mathrm{s} = 0.4$, represented by the dotted line.

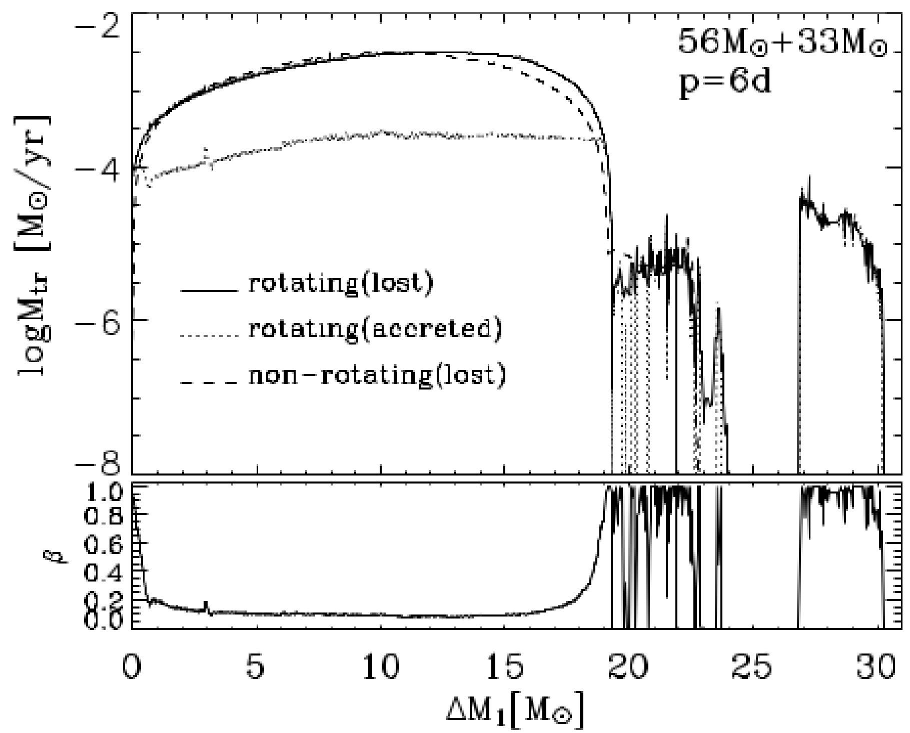

Fig. 21. *Upper plot*: mass transfer (solid line) and accretion rate (dotted line) of the rotating initial system $56\,M_\odot + 33\,M_\odot$, $p = 6$ days. Dashed line represent mass transfer rate in the corresponding non-rotating binary. *Lower plot*: accretion efficiency of the secondary taking into account matter lost by the primary only due to mass transfer.

Petrovic, Langer, van der Hucht, 2005

Massive binary evolution example – internal structure

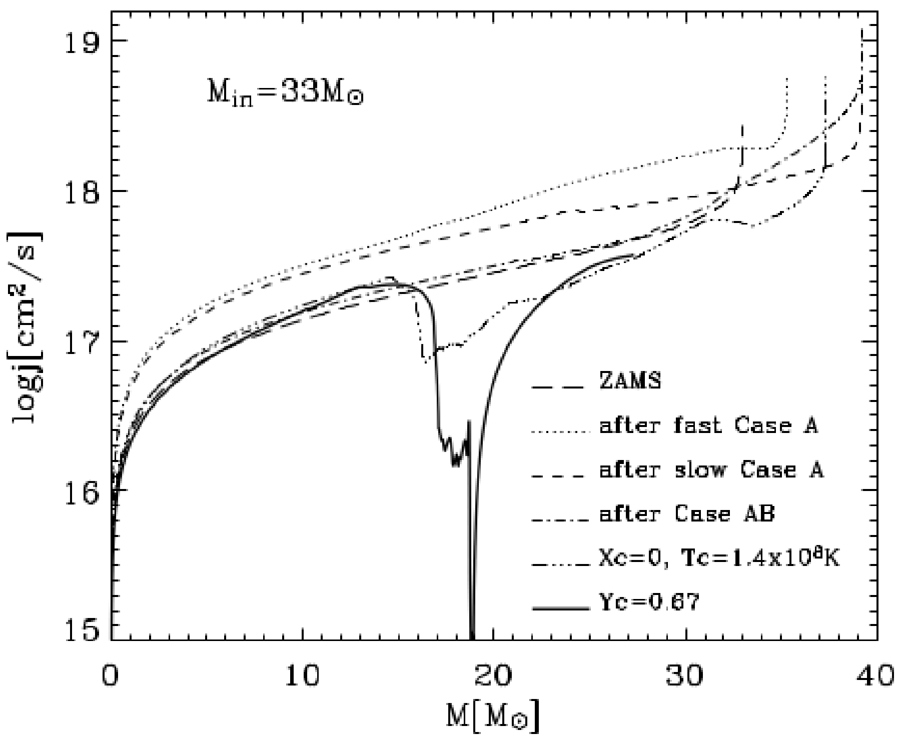

Fig. 11. Specific angular momentum profiles of the secondary star on the hydrogen ZAMS (long dashed line), after fast (dotted line) and slow (short dashed line) Case A mass transfer, after Case AB mass transfer (dash-dotted line), when helium ignites in the core (three dots-dashed line) and when the central helium abundance is 67% (solid line).

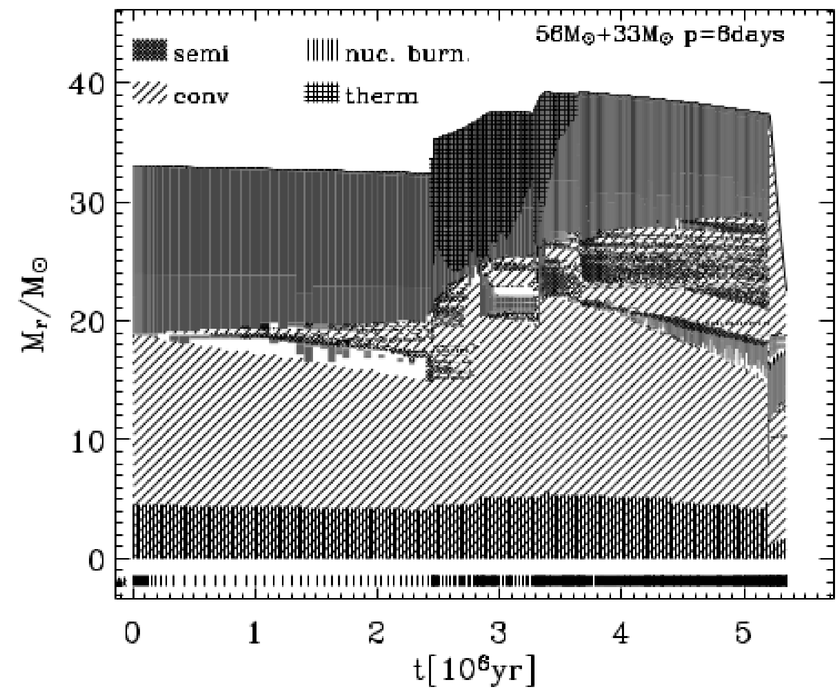

Fig. 7. Evolution of the internal structure of a rotating 33 $M_\odot$ secondary from the ZAMS until red supergiant phase $Y_c = 0.67$. Convection is indicated with diagonal hatching, semiconvection with crossed hatching and thermohaline mixing with straight crossed hatching. The hatched area at the bottom indicates nuclear burning. Gray shaded areas represent regions with rotationally induced mixing (intensity is indicated with different shades, the darker the colour, the stronger rotational mixing). The topmost solid line corresponds to the surface of the star.

Petrovic, Langer, Yoon & Heger, 2005

MESA - Modules for Experiments in Stellar Astrophysics

(Paxton et al. 2011, 2013, 2015, 2018, University Santa Barbara US)

*Hydrodynamic stellar evolution code, calculates simultaneously evolution of both stellar components in a circular orbit and the mass transfer
*Nuclear reaction library includes more than 300 rates for elements up to nickel (Caughlan & Fowler 1988, Augulo et al. 1999)
*Includes convection, overshooting, semiconvection and thermohaline mixing
*Opacity tables (Cassisi et al. 2007)
*Stellar wind mass loss included (various option depending on stellar mass and phase: Vink et al 2001 for O and B stars, de Jager, Nieuwhuizen & van der Hucht 1988 for MS, Kudritzki 1989 for massive MS stars, Nugis & Lamers 2000 for WR stars, "Dutch" all authors for massive stars, Reimers 1975 for red giants, Blocker 1995 for AGB stars...)
*Rotation is derived from STERN (Heger, langer & Woosley 2000, Heger, Woosley & Spruit, application in binaries Petrovic et al. 2005; Yoon & Langer, 2005)
*Rotationally induced mass loss also from STERN (Langer 1998)
*Transport of angular momentum and chemicals due to rotationally-induced instabilities is implemented in a diffusion approximation, the same like in STERN (e.g., Endal & Sofia 1978; Pinsonneault et al.1989; Heger et al. 2000)
*Spruit-Tayler dynamo in MESA is based on STERN (Petrovic et al. 2005) and KEPLER (Heger et al. 2005)

MESA binary module

(Paxton et al. 2011, 2013, 2015, 2018)

-Mass transfer rate through the first Langrangian point as in STERN (Ritter 1988)
-Accretion efficiency control (Tauris & van der Heuvel 2006)

-Evolution of Orbital angular momentum: mass loss, magnetic braking, spin-orbit coupling (for rotating models) and gravitational waves:

Mass lost in a stellar wind has the specific orbital angular momentum of its star (Sobberman et al. 1997)

Spin-down of a star due to a magnetic field (Rappaport et al. 1983, Verbunt & Zwaan 1981)

Tidal interaction and mass transfer can significantly modify the spin angular momentum of the stars in a binary system (Hut 1981, Hurley 2002, Detmers et al. 2008)

Compact binaries can experience significant orbital decay due to the emission of gravitational waves and the angular momentum loss (Weisberg & Taylor 2005, Kramer et al. 2006) https://docs.mesastar.org/

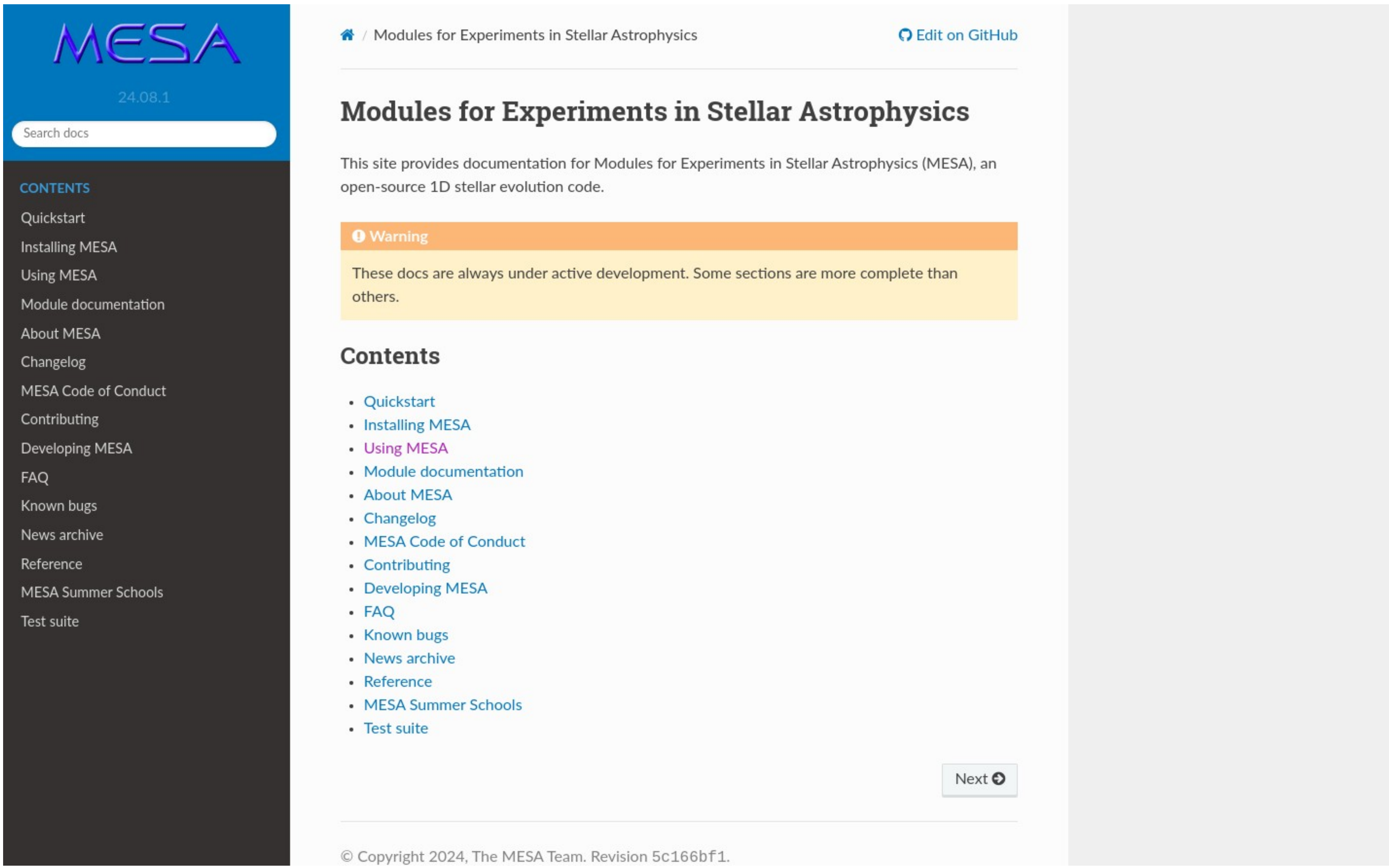

MESA

24.08.1

Search docs

CONTENTS

- Quickstart
- Installing MESA
- Using MESA
- Module documentation
- About MESA
- Changelog
- MESA Code of Conduct
- Contributing
- Developing MESA
- FAQ
- Known bugs
- News archive
- Reference
- MESA Summer Schools
- Test suite

/ Modules for Experiments in Stellar Astrophysics

Edit on GitHub

Modules for Experiments in Stellar Astrophysics

This site provides documentation for Modules for Experiments in Stellar Astrophysics (MESA), an open-source 1D stellar evolution code.

Warning

These docs are always under active development. Some sections are more complete than others.

Contents

Next

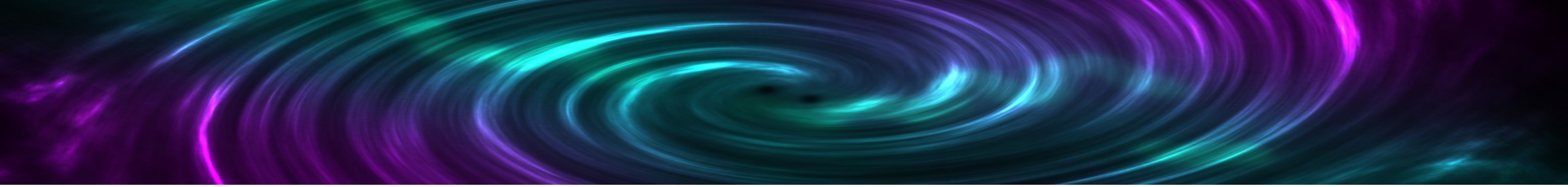

MESA output files

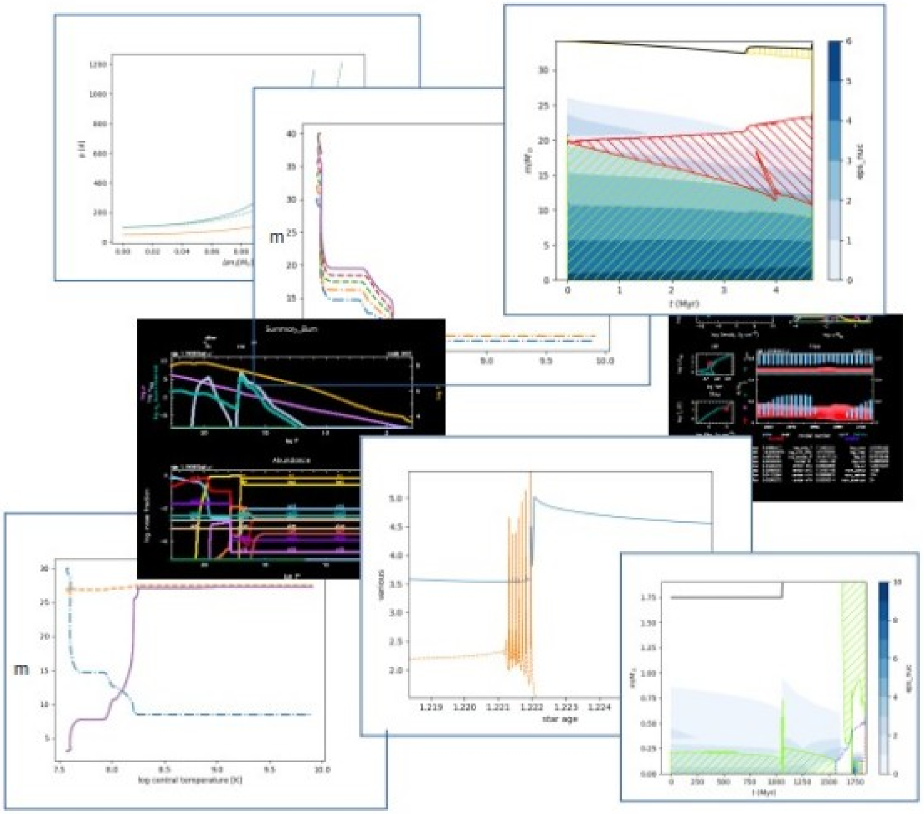

MESA code will generate three main type of datasets:

Datasets with details of evolution of stellar structure for each star in a binary system: star age, mass, radius, effective temperature, total luminosity, central temperature, central density, central pressure, stellar wind mass loss, the mass of the convective core, the mass of helium, carbon, oxygen, silicon and iron core, various mixing coefficients, central and surface abundances of hydrogen, helium, carbon and oxygen isotopes etc.

Datasets with details of orbital evolution of the bnary system: stellar masses, radii, Roche radii, orbital period, separation, orbital velocities of stars, mass transfer rate, mass accretion rate, angular Momentum etc.

Datasets with detailed information about the interior structure of star, one file per time step. Each file contains a set of properties of the star, from the center to the surface: mass, radius, temperature, pressure, hydrogen mass fraction, helium mass fraction, metalicity, energy from nuclear reactions etc.

Population synthesis models of GW

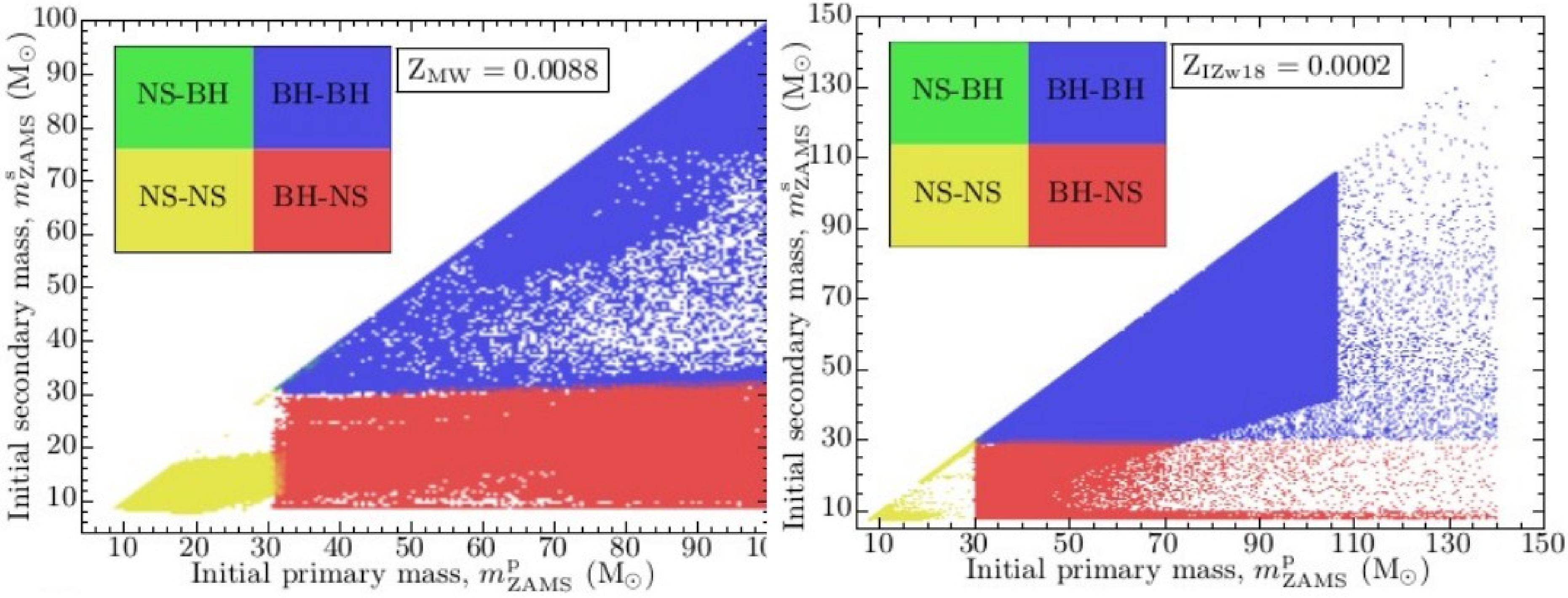

Kruckow et al. 2018

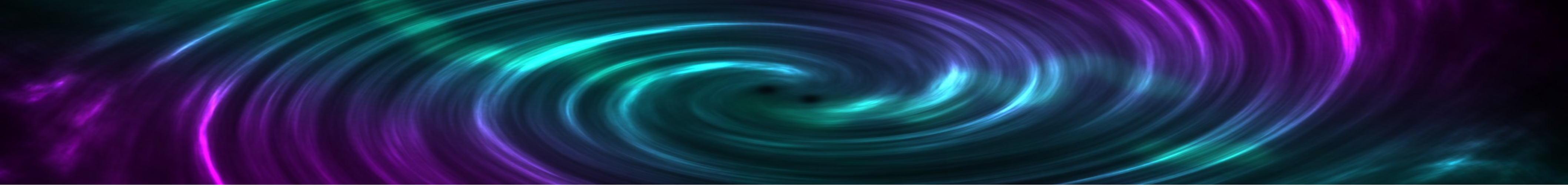

Preliminary results – initial period - masses 30-40 M☉

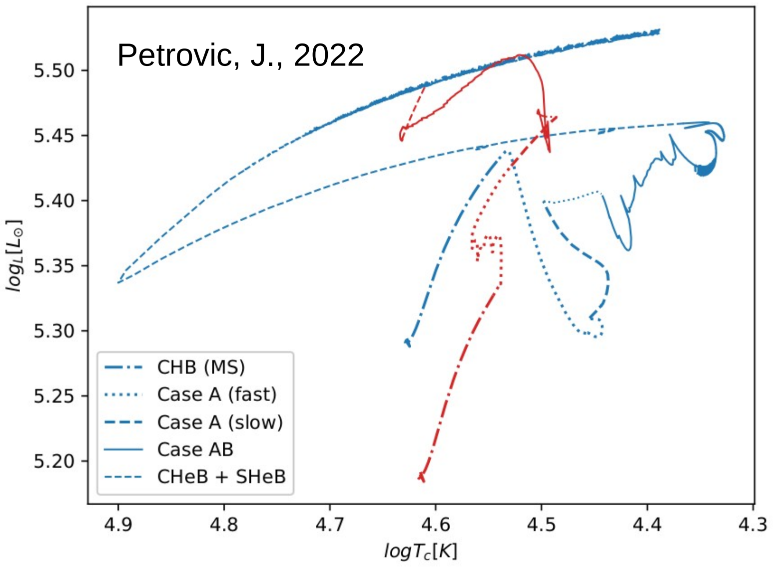

Fig. 1. *The evolutionary tracks of the primary (blue line) and the secondary star (red line) in $37.0M_\odot + 33.3M_\odot$ binary system with an initial orbital period of 3 days.*

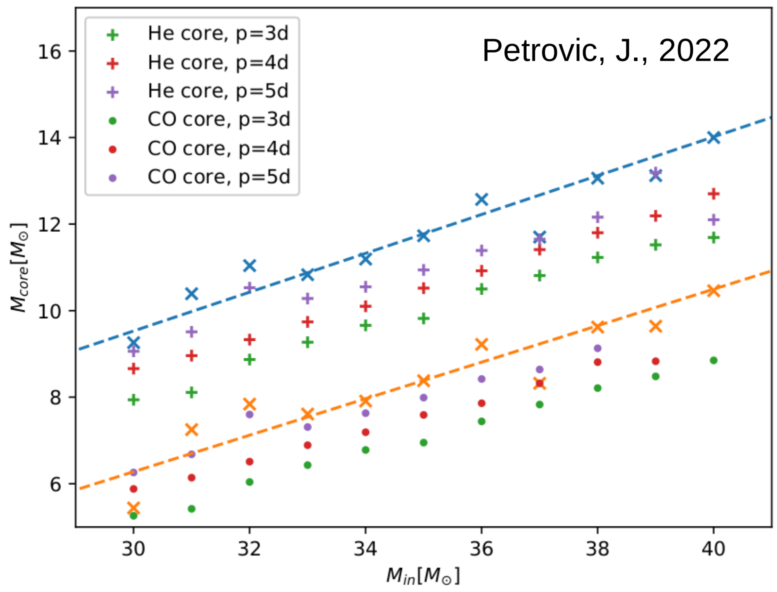

Fig. 2. *Helium and carbon-oxygen core masses as a function of the initial stellar masses for primaries. The dashed lines represent linear fits for single stars.*

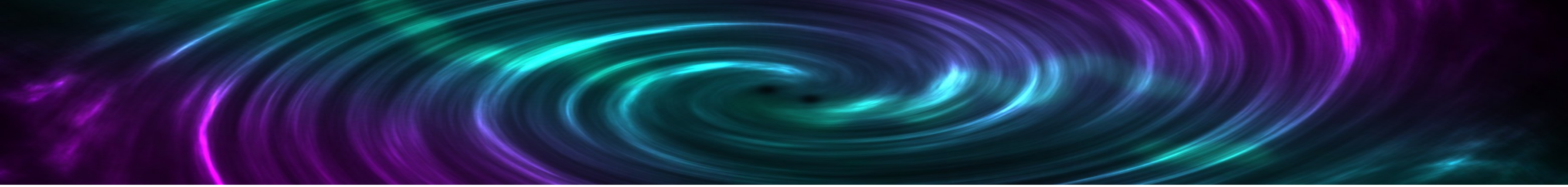

Preliminary results – metalicity - masses 30-40 M☉

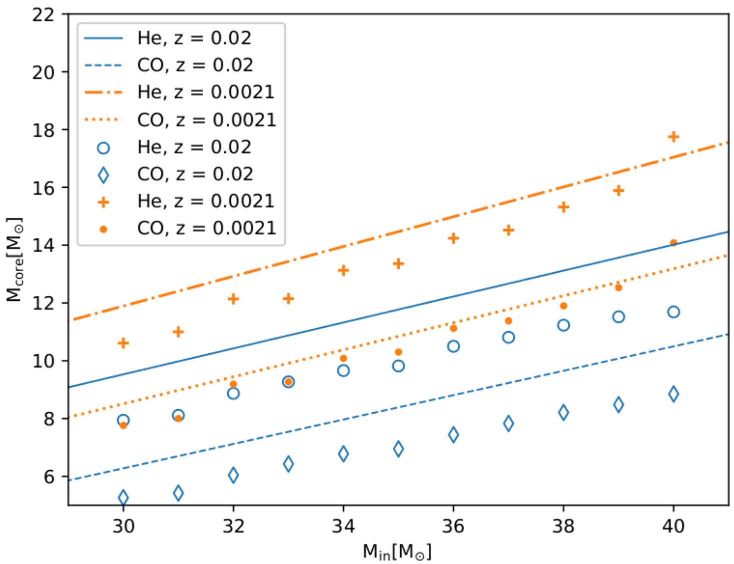

Fig. 4: The mass of the He and CO core for binary systems with the initial orbital period of 3 days for metallicity $z = 0.02$ and $z = 0.0021$ as a function of initial mass. The lines represent linear fits for single stars for both metallicities.

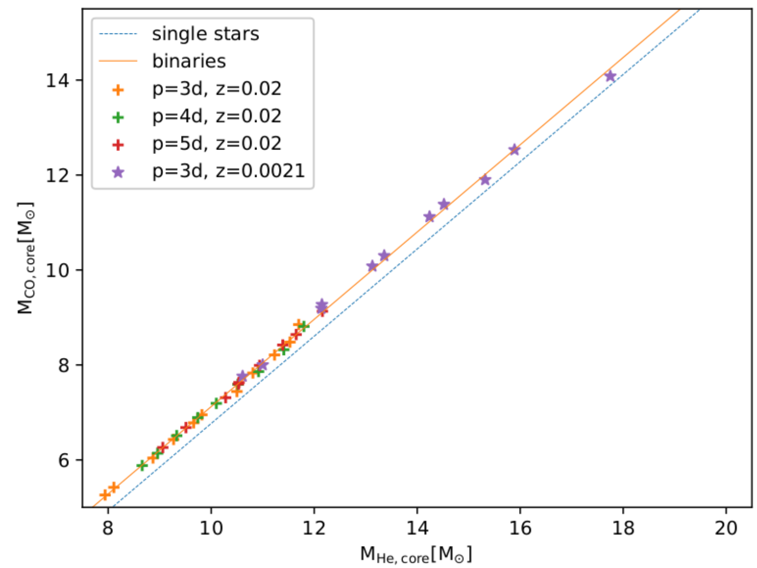

Fig. 5: The mass of the He and CO core for binary systems with an initial orbital period of 3, 4 and 5 days for metallicity $z = 0.02$ (Petrovic 2022) and an initial orbital period of 3 days for $z = 0.0021$ from this paper. The solid line represents the fit for all binary systems and the dashed line for all single star models.

Petrovic, J., 2023

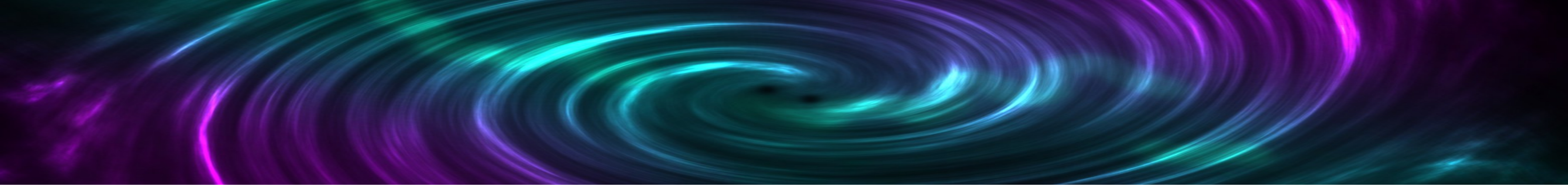

Convective – Kippenhahn plots: internal structure evolution

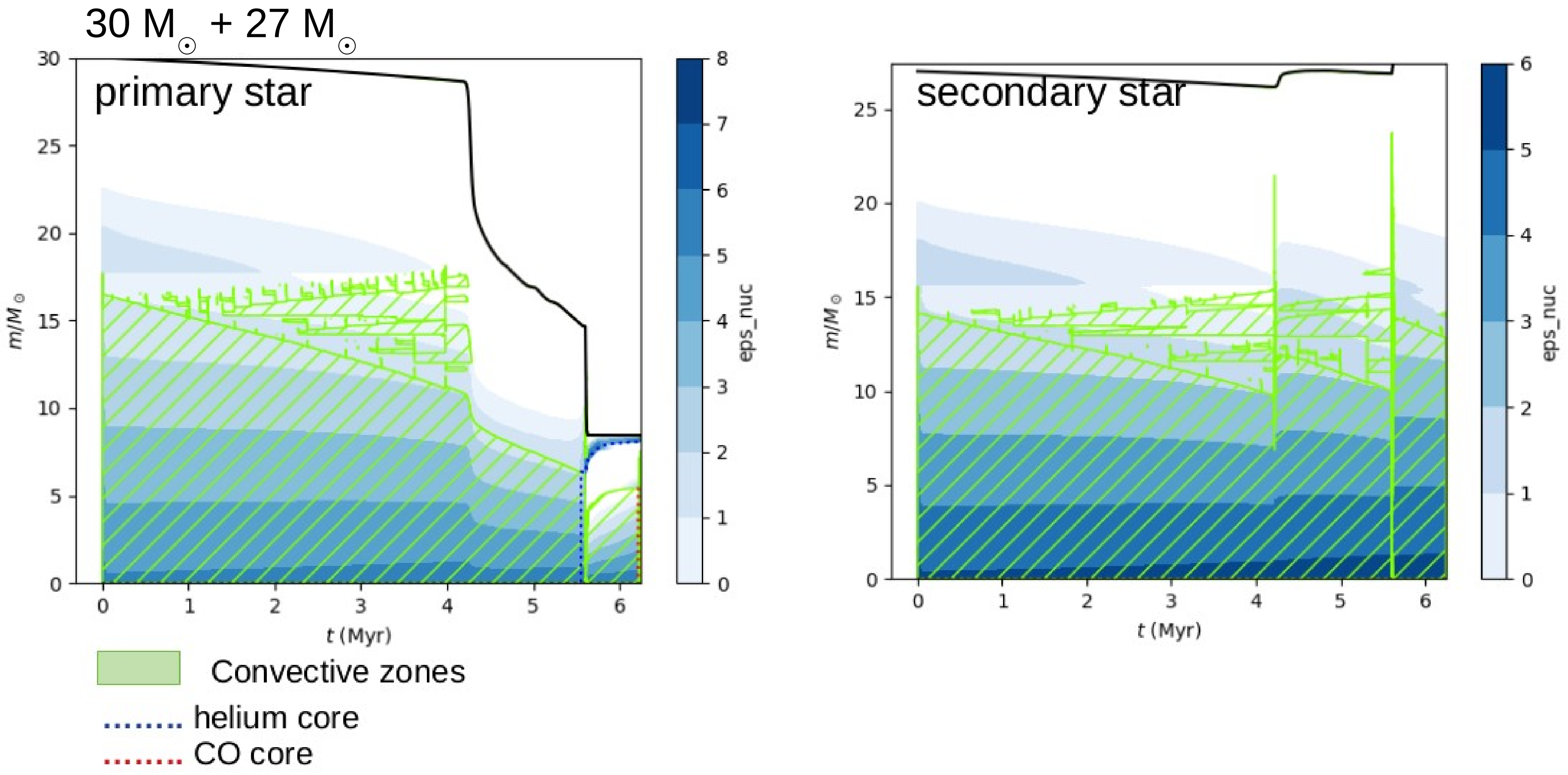

Preliminary results - masses 30-40 M☉

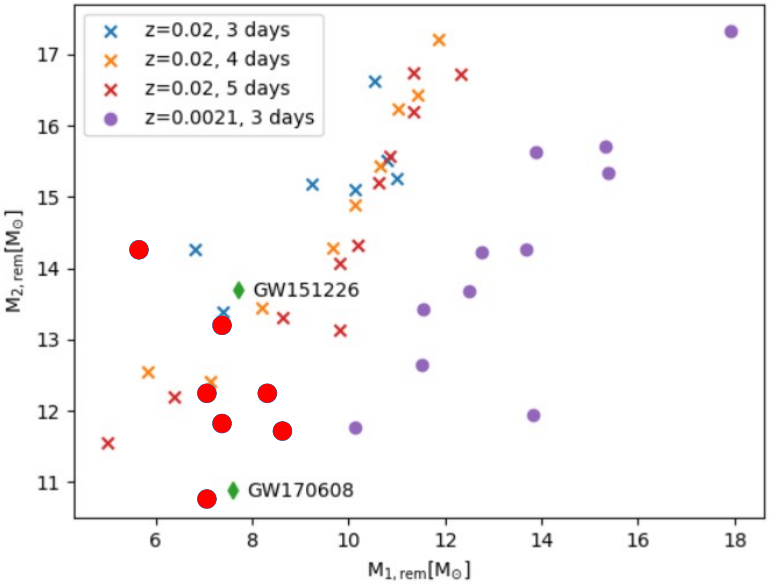

Figure 2. The mass of BHs for highly non-conservative binary systems with the initial orbital period of 3, 4 and 5 days for metallicity z = 0.02 (marked with x) and the initial orbital period of 3 days and z = 0.0021 (marked with circles).The observed GW sources are marked with diamonds .

MOBY models (z =0.02)

Rotating super-massive Case A binary systems with the solar metallicity were obtained with the MESA (Modules for Experiments in Stellar Astrophysics) code (Paxton et al. 2011, 2013, 2015, 2018) in revision 10398. The evolution was calculated to the first carbon-oxygen (CO) core formation in the system.

Shellular rotation was implemented BY Meynet & Maeder (1997) with modifications of the stellar equations based on Kippenhahn & Thomas (1970).

Transport of the angular momentum and chemicals is implemented in a diffusion approximations for rotationally induced mixing processes: dynamical shear instability, Solberg – Hoiland instability, secular shear instability, Eddington – Sweet circulation and Goldreich – Schubert – Fricke instability.

Rotationally induced mass loss is included as proposed in Langer (1998).

Rotation of both components is synchronized with the orbital period and the orbit is assumed to be circularized.

Ritter (1988) scheme is used for the calculation of mass transfer rate and the composition of accreted material is the same as the donor’s current surface composition.

Model with the stellar winds according to Vink et al. (2001) and Nugis and Lamers (2000) for the Wolf-Rayet phase were compared with the model where scaling factor of 0.1 and 0.5 were included.

MOBY models example (z = 0.02)

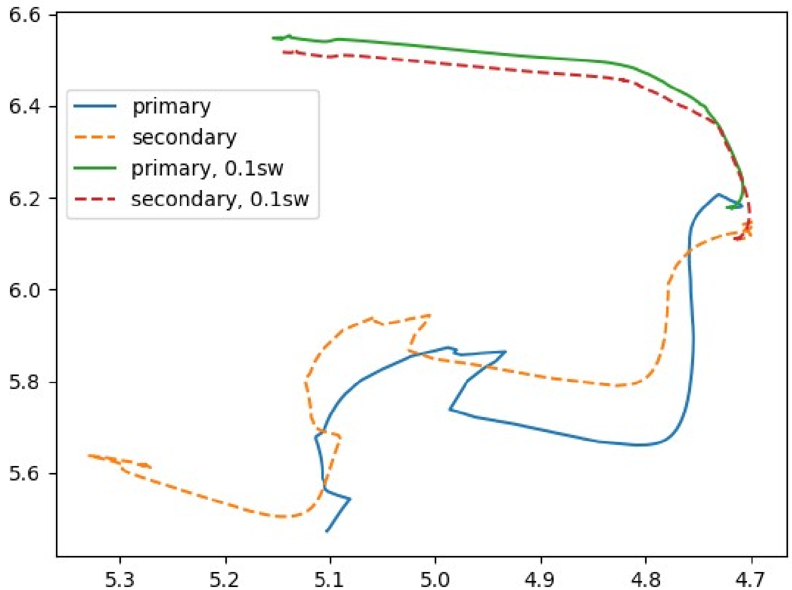

Petrović, Jurković, Arbutina, Čeki, Đurašević, EAS 2024

The initial configuration 110 + 100 Ms, orbital period of 3 days
Model with the stellar winds according to Vink et al. (2001) and Nugis and Lamers (2000) for the Wolf-Rayet phase were compared with the model where scaling factor of 0.1 was included.

Large difference was found in the evolution of these two models. Due to the extremely high stellar wind mass loss rate and rotationally enhanced mass loss, in the first model, the final stellar masses (final helium core mass, as there is no hydrogen envelope left) are just above 12 Ms and CO core masses are very low, just under 10 Ms, which would results in black hole (BH) remnants of about 11Ms (Belczynski et al. 2008, 2010). Also, in this model, the secondary star forms CO core first and is the one that will first explode as a supernova. The orbital period at the moment of the first supernova explosion is above 180 days.

In the second model, with significantly higher total and CO core masses of about 70 and 60 Ms respectively (for the primary star 70.5 Ms and 62.3 Ms, which is in excellent agreement with the relation between the final helium core mass and CO core mass derived in Petrovic 2022), final double BH masses would be about 65 Ms and the presupernova explosion orbital period is just above 6 days.

MOBY model examples

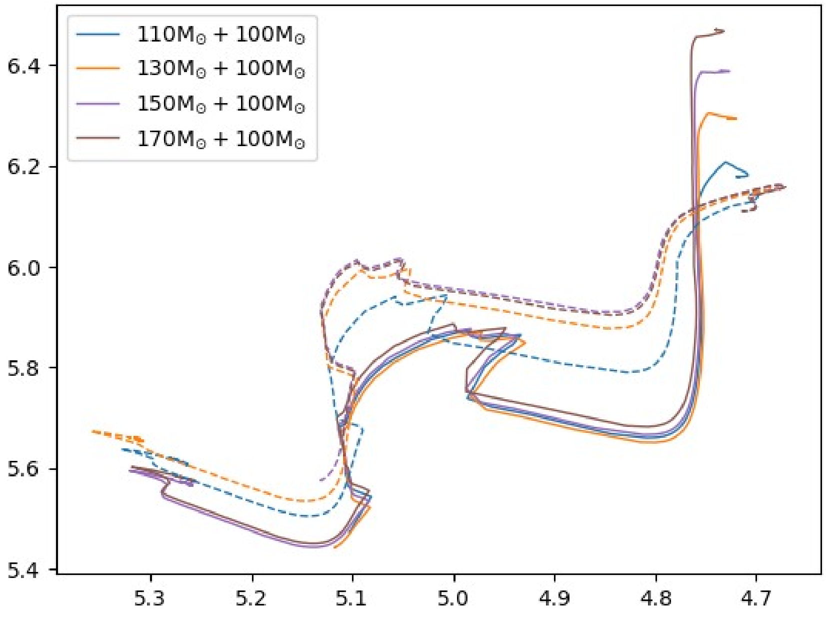

Petrović, Jurković, Arbutina, Čeki, Đurašević, IAU 2024

Stellar wind scaling 1, initial period 3 days

Evolutionary tracks of binary systems with the initial orbital period of 3 days and the initial masses of the primary star of 110, 130, 150 and 170 Ms, while the secondary is 100 Ms in all models.

It is visible that the evolutionary tracks for all primary stars are very similar and ,while they start on different places of Zero Age Main Sequence (ZAMS), they all end on almost the same point.

Due to high stellar wind mass loss rate and extreme rotationally induced mass loss, all primary stars end up without hydrogen envelopes with carbon-oxygen (CO) core masses of about 10 Ms and total masses of about 12 Ms.

According to (Belczynski et al. 2008, 2010), **black hole remnant masses of such stars would be just above 10 Ms.**

The orbital period at the moment of the first supernova explosion for those models are about 180-240 days.

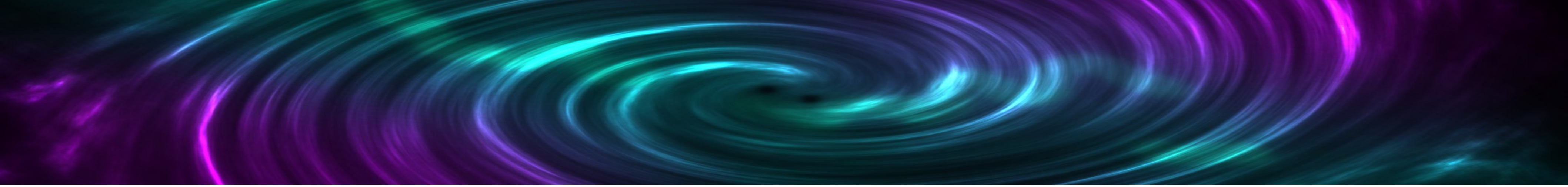

MOBY model examples

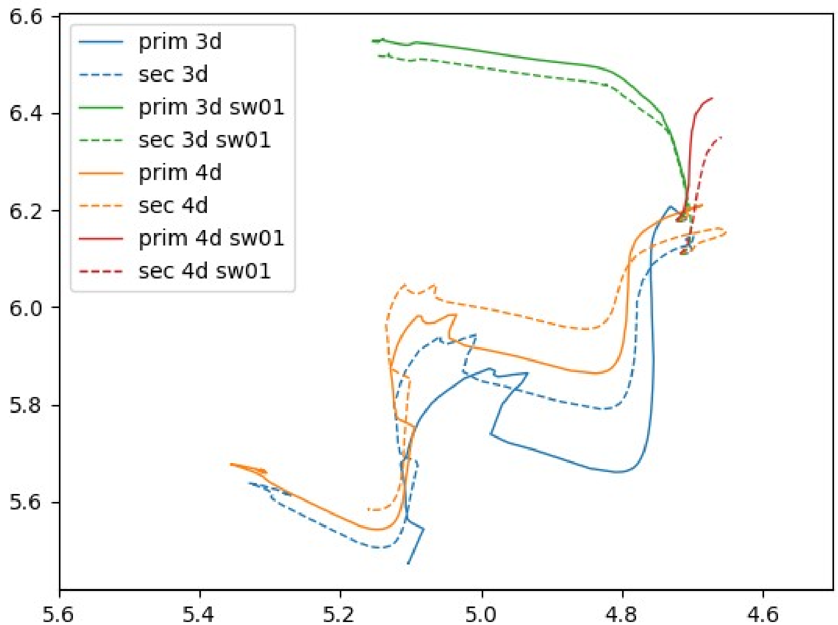

Petrovic, Jurkovic, Arbutina, Čeki, Đurašević, IAU 2024

Stellar wind scaling 1 and 0.1, initial periods 3 and 4 days

For the initial orbital period of 4 days and non-scaled stellar wind mass loss rate, **the resulting CO core mass is about 10 Ms and the presupernova orbital period is about 210 days**, so slightly wider initial orbit results in about the same primary CO core mass and somewhat broader final configuration.

However, scaling stellar wind to 0.1 of its value leads to a totally different evolution of this binary system: **contact between two stellar components.**

Remnant masses – primary stars

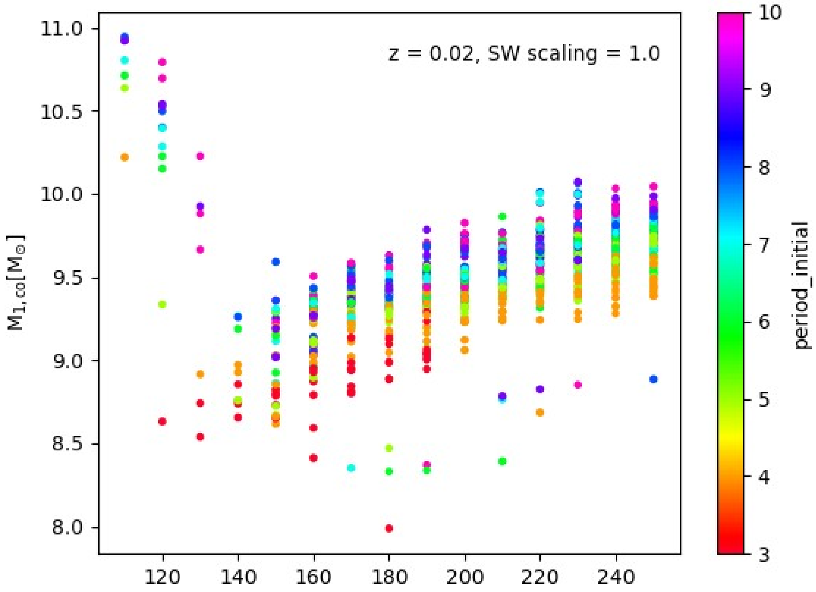

- -3000 systems with Solar metallicity
- -rotation included
- -initial masses 100 – 250 $M_\odot$
- -initial periods 3-10 days
- -SW scaling 1, 0.5 and 0.1

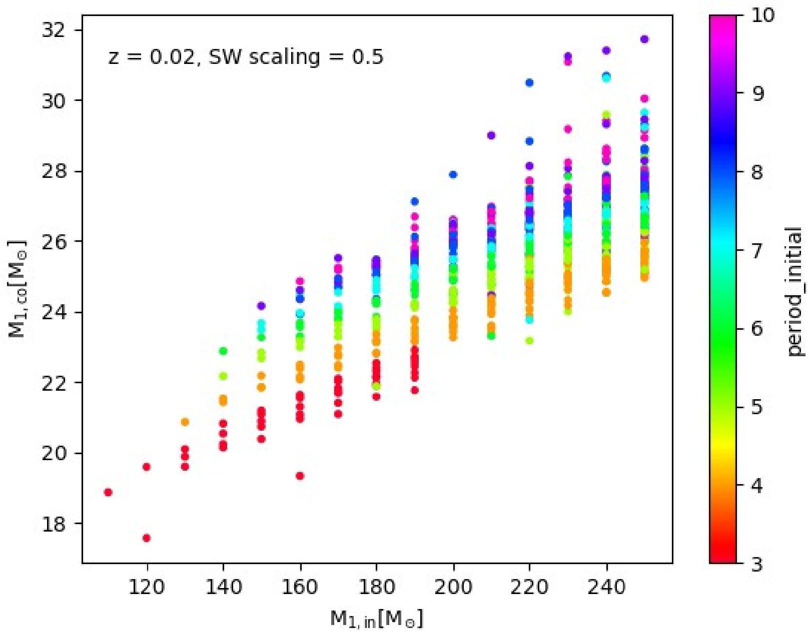

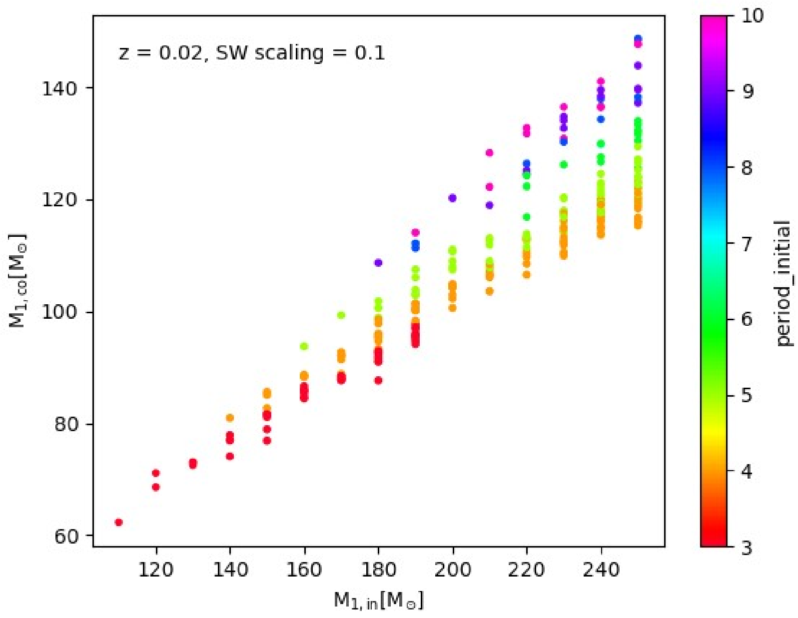

Presupernova orbital periods

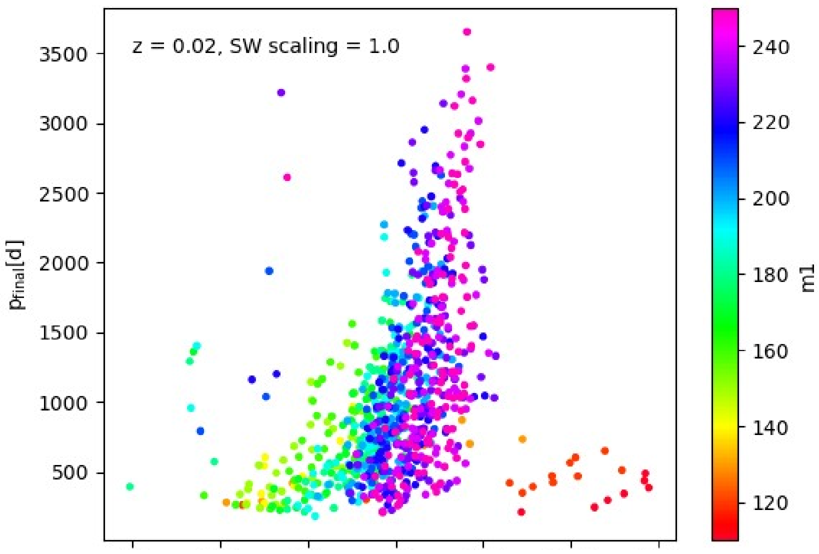

-3000 systems with Solar metalicity
-rotation included
-initial masses 100 – 250 $M_\odot$
-initial periods 3-10 days
-SW scaling 1, 0.5 and 0.1

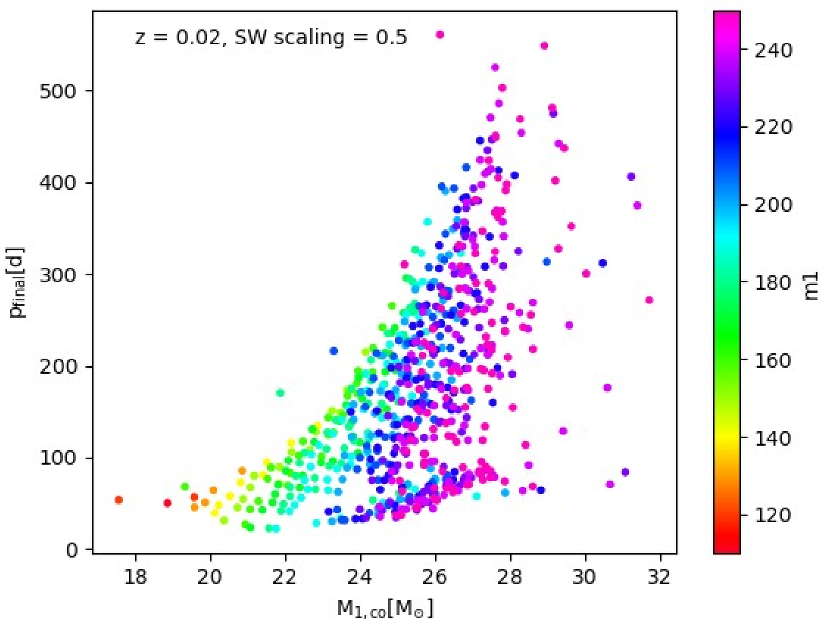

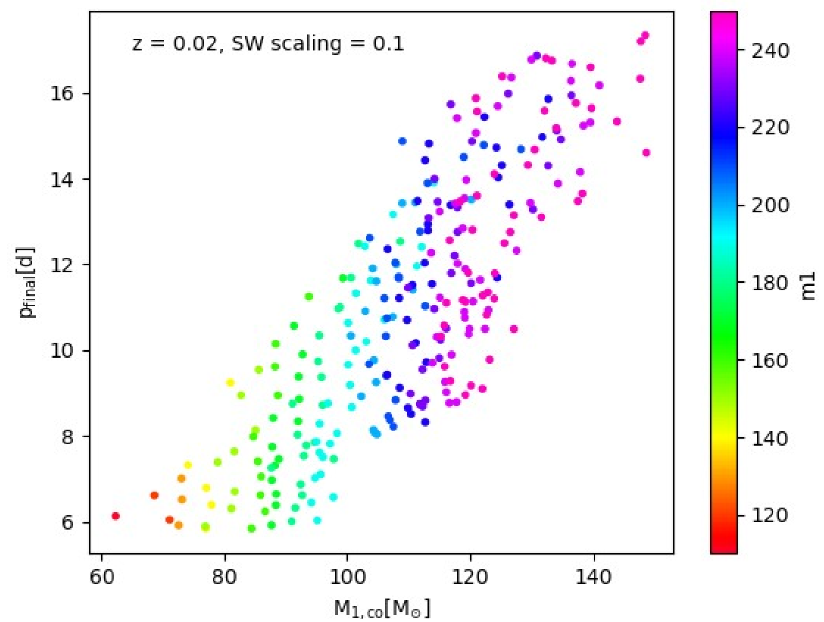

Pair-instability Supernovae (B. Arbutina, N. Mladenović)

-It is currently suggested that supermassive stars with lower metallicity reach a stage where a pair-instability supernova occurs.

-Production of free electrons and positrons temporary decreases the internal pressure, supporting a supermassive star's core against gravitational collapse.

-The pressure drop afterwards leads to a star being blown apart without leaving a remnant.

-Pair-instability supernovae can only happen in stars with a mass range from around 130 to 250 solar masses and low to moderate metallicity.

-The initial mass limit for pair instability depends on the metallicity and rotation properties. For binary systems, the initial configuration of the system has to be also taken into account.

Neural network approach (A. Mitrašinović)

- Train a deep neural network (DNN) to predict the evolution of modeled binary systems.

- Use the trained neural network to facilitate the extension of the existing database.

- Extend the neural network to infer the progenitor properties from the system observables

Conclusions and future steps

Proposal was for total 1000 models, we have already 3000 models with Solar metalicity → large dependence of remnant masses and pre-supernova orbital periods on the stellar wind mass loss rate
-secondaries to be evolved to PSN

-1000 models with SMC (0.0021) metalicity
-1000 models with Zwicky 18 (0.0004) metalicity

-point star + secondary models (most likely common envelope evolution)
-SN MESA module tests

-Pair-instability supernova
-Neural network approach

-All models to be available online

Radna stanica

Čisto poređenja ja sam juče spremio cenu sa 1024GB RAM i 3 hard diska.
Možda se i uklopi, ako ne, smanjićemo nešto.

QTY	Prod #	Product Description	PL	Cena bez PDV-a
1	4Y2D2AV	HP Z8 TWR G5 1450W 200V/10A EPA90 RCTOBU	5X	13.280,00 €
1	4YQ39AV	OS Localization	5X	
1	3F4J0AV	HP Linux-ready	5X	
1	3F4K4AV	OS Load to M.2	5X	
1	6N8Q4AV	Intel Xeon 6430 32C 270W CPU	5X	
1	6N8Q5AV	Intel Xeon 6430 32C 270W 2nd CPU	5X	
1	3F4M2AV	1TB(16x64GB)DDR5 4800 DIMMECCREG2CPU Mem	5X	
1	616D1AV	NVIDIA T400 4GB 3mDP GFX	5X	
1	3F3A6AV	ZTrb 1TB PCIe 2280 TLC M.2 SSD	5X	
1	3F4G2AV	8TB 7200 SATA Enterprise 3.5in	5X	
1	3F4G3AV	8TB 7200 SATA Enterprise 3.5in 2nd	5X	
1	3F4G4AV	8TB 7200 SATA Enterprise 3.5in 3rd	5X	
1	3F4Q4AV	HP USB 320K KB	5X	
1	3F4J3AV	HP WRD 320M Mouse	5X	
1	3F4K2AV	9.5 DVDWR 1st ODD	5X	
1	6U7A8AV	Type-A SprSpd USB 5Gbps FrntIOv2EntryMod	5X	
1	6Z327AV	1/1/1 Warranty	5X	
1	63G43AV	C13 stkr CNVTL WKS Power Cord	5X	
1	3F0V6AV	No Adapters Needed	5X	
1	3F2Z2AV	Data Science Ready	5X	
1	3F4J2AV	Single Unit (TWR) Packaging	5X	
1	3F3D9AV	Z8 Country Kit	5X	
1	7M3R8AV	1/1/1 TWR LBL	5X	
1	AY130AV	HP Packaging Tag Service	9R	
1	766U7AV	HP Packaging Tag SN+MAC1+UUID+PKID SVC	9R	
1	ZD081AA	HP standard delivery (Door/Dock) WS	16	
1	U61CFE	HP 3y Onsite Care w/DMR WS HW Supp	MG	50,00 €

Cena adekvatnog UPS uređaja ne bi trebalo da pređe 2000€+pdv

Binary systems – basics

The **primary** star in a binary system, the component with the greater mass, evolves faster than the **secondary** and through envelope expansion may reach the radius of its Roche lobe and start **transfering mass** onto the secondary star through the first Lagrangian point. This process is also called **Roche lobe overflow** (RLOF).

The Roche lobe is a volume around each star in a binary system, inside which material is bound to that star. If the star expands past its Roche lobe, then the material outside of the lobe will fall into the other star. The potential energy is calculated in a frame of reference that corotates with the binary system.

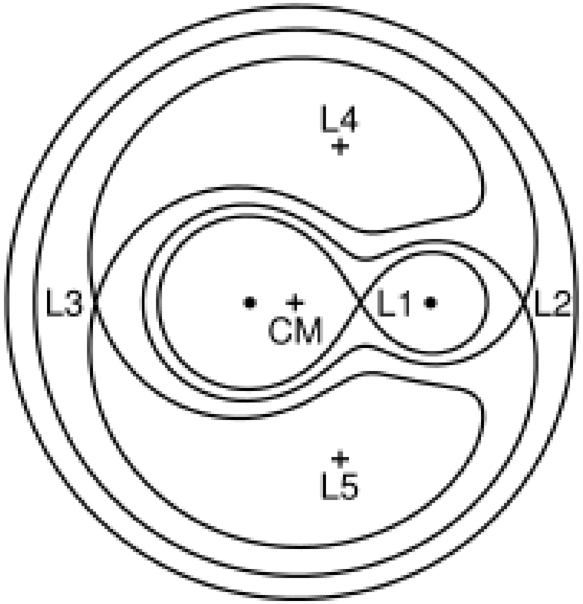

Close to each star, surfaces of equal gravitational potential are approximately spherical and concentric with the nearer star. Far from the stellar system, the equipotentials are approximately ellipsoidal and elongated parallel to the axis joining the stellar centers. A critical equipotential intersects itself at the L1 Lagrangian point of the system, forming a two-lobed figure-of-eight with one of the two stars at the center of each lobe. This critical equipotential defines the Roche lobes.

Different types of mass transfer in binary systems

Depending of the value of the initial period of a binary system, the primary will fill its critical radius (Roche) during different phases of evolution:

Case A:
initial orbital period is in the order of days – occurs while the primary is still a main sequence star – two phases: fast on thermal time scale and slow on nuclear time scale

Case B:
initial binary period is in order of weeks – occurs when the helium core of the primary is contracting and the shell hydrogen burning envelope is expanding – thermal time scale, shorter than in Case A

Case C:
initial period is in the order of months or years – occurs when the primary fills its Roche lobe during helium shell burning - dynamical time scale

Massive binary evolution example – internal structure

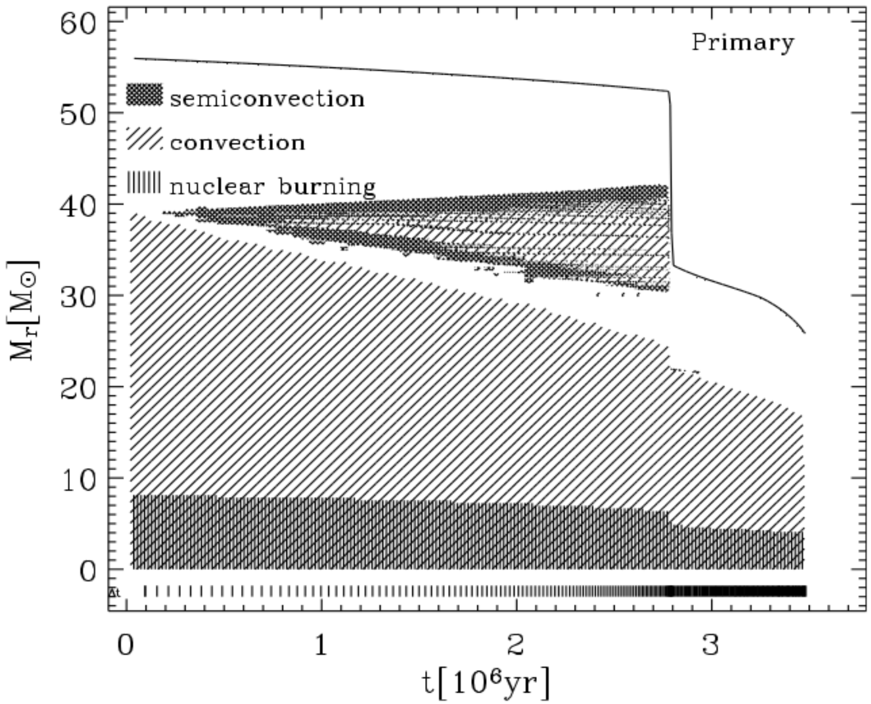

Fig. 4. The evolution of the internal structure of the 56 $M_\odot$ primary during the core hydrogen burning. Convection is indicated with diagonal hatching and semiconvection with crossed hatching. The hatched area at the bottom indicates nuclear burning. The topmost solid line corresponds to the surface of the star.

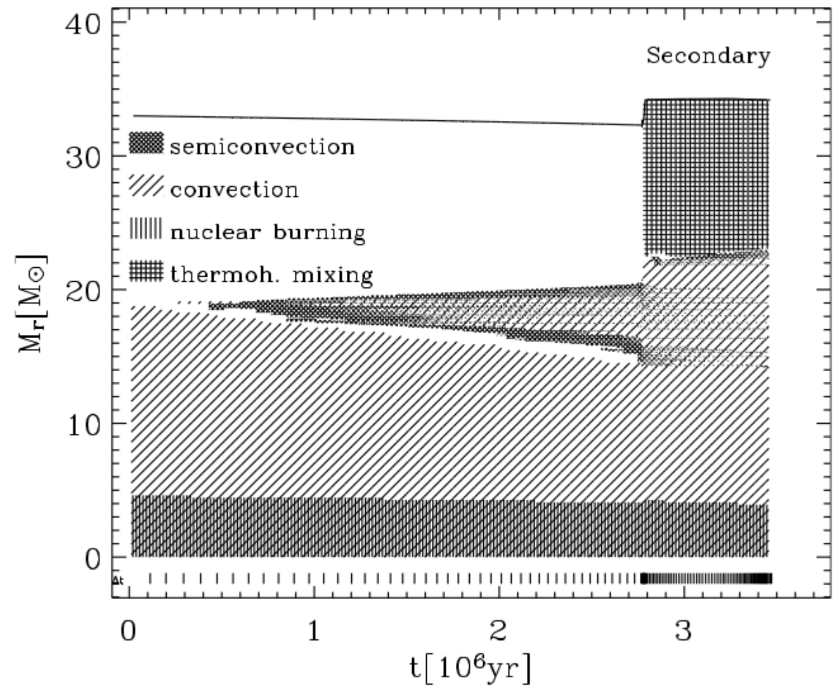

Fig. 5. The evolution of the internal structure of the 33 $M_\odot$ secondary during core hydrogen burning of the primary. Convection is indicated with diagonal hatching, semiconvection with crossed hatching and thermohaline mixing with straight crossed hatching. The hatched area at the bottom indicates nuclear burning. The topmost solid line corresponds to the surface of the star.

Petrovic, Langer, van der Hucht, 2005

Our rotating models – in which the accretion efficiency is no free parameter any more but is computed selfconsistent and time-dependent – reproduce the observed WR+O binaries quite well, as good as our models without rotation physics, where the accretion efficiency is a free parameter.

The accretion efficiency during the major mass transfer phase in the progenitor evolution of the three observed WR+O binaries is small, i.e. $\beta = 0...0.1$, as for larger β the O stars during the WR+O phase are more massive and the WR/O-mass ratios smaller than observed. However, it is unlikely that the secondaries did not accrete at all ($\beta = 0$), since some O stars are found to rotate faster than synchronously.

The initial orbital period needs to be larger than $\sim$3 days, to avoid contact at the beginning of hydrogen burning and obtain massive enough WR stars and should be shorter than the observed orbital periods in the three WR+O systems, i.e. shorter than $\sim$10 days. This excludes Case B mass transfer.

While the initial mass ratio should not be too far from unity so contact is avoided, it should be close to the contact limit, since this leads to the shortest orbital periods and largest WR/O mass ratios in WR+O systems, as needed for the three observed systems.

STERN evolutionary code

(Braun 1998 and further Langer, Wellstein, Heger, Petrovic,Yoon, Cantiello)

-hydrodynamic stellar evolution code
-calculates simultaneously evolution of both stellar components in a circular orbit and the mass transfer within the Roche approximation (Kopal 1978)
-mass transfer rate through the first Langrangian point (Ritter 1988)
-stellar wind mass loss for O stars on the main sequence (Kudritzki et al 1989) and for WR stars Hamman et al (1995).
-changes in chemical composition are computed using a nuclear network including pp chains, the CNO-cycle, and the major helium, carbon, neon and oxygen burning reactions.
-includes convection, semiconvection (Langer 1991, Braun & Langer 1995)
-OPAL Rosseland mean opacities (Iglesias & Rogers 1996)
-change of orbital period due to mass transfer (Podsiadlowski 1992)
-synchronization due to tidal spin-orbit coupling (Zahn 1977)
-rotationally enhanced mass loss (Langer 1998)
-rotationally induced mixing processes (Heger 2000)
-magnetic field generated due to differential rotation (Spruit 2002)

Collapsars and Gamma-ray Bursts

*Collapsar is a massive (M >35−40Ms, Fryer 1999) rotating star whose core collapses to form a black hole (Woosley 1993b; MacFadyen & Woosley 1999).

*If the collapsing core has enough angular momentum ($j \geq 3 \times 10^{16} cm^2 s^{-1}$, MacFadyen & Woosley 1999) an accretion disk is formed around the black hole.

*The accretion of the rest of the core at accretion rates up to 0.1 Ms/s by the newly-formed black hole can produce a collimated highly relativistic outflow.

*In case the star has no hydrogen envelope, a GRB accompanied by a type Ib/c supernova may be produced.

The collapsar models for GRB need three ingredients:
-a massive core
-loss of the hydrogen envelope
-sufficient angular momentum to form an accretion disk

How to make collapsar - Binary stars

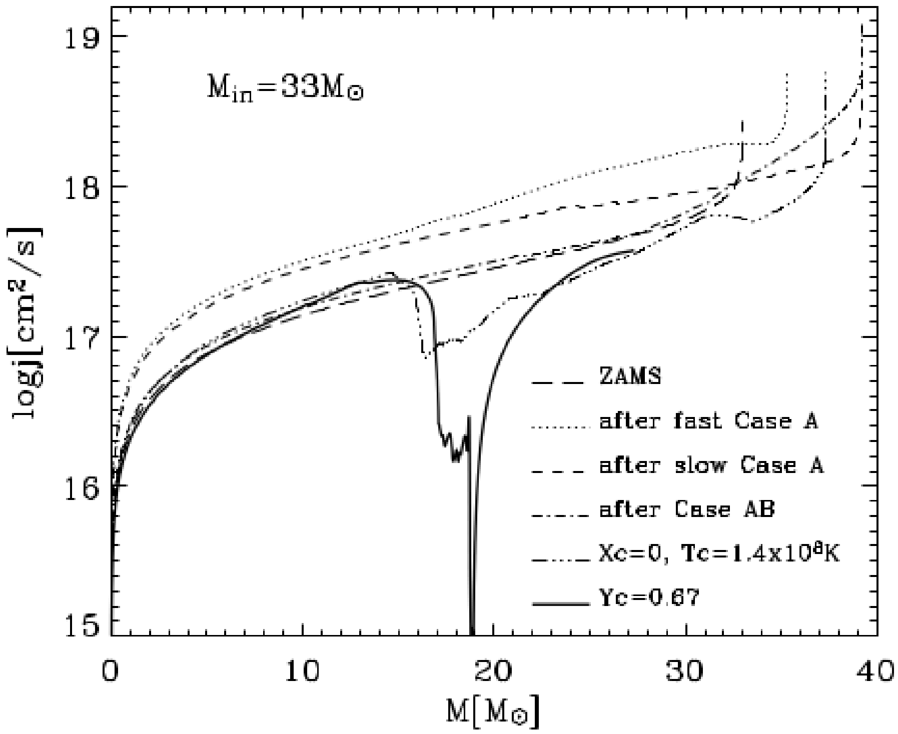

Fig. 11. Specific angular momentum profiles of the secondary star on the hydrogen ZAMS (long dashed line), after fast (dotted line) and slow (short dashed line) Case A mass transfer, after Case AB mass transfer (dash-dotted line), when helium ignites in the core (three dots-dashed line) and when the central helium abundance is 67% (solid line).

56Ms+33Ms, p=6d

Models include the inhibiting effect of μ-gradient on rotationally induced mixing processes

The binary system synchronizes during MS
Vsurf,2= 64km/s (compared to 200km/s for the single star)
Stellar wind mass loss of the secondary is $\sim 10^{-7}$Ms/yr

The secondary accretes ~3 Ms during the fast phase and ~4 Ms during the slow phase of Case A mass transfer
→ Vsurf,2~ 200km/s

The secondary accretes ~0.25 Ms during Case AB mass Transfer → Vsurf,2~ 500km/s

When the secondary spins up to close to critical rotation it loses more mass and is also spun-down by tidal forces that try to synchronize it with the orbital motion

At the end of core helium burning and carbon as well, angular momentum of the presupernova core (3 Ms) Is **4×10^{16}cm^{2}s^{-1} → GRB!**

Petrovic, Langer, Yoon & Heger A&A, 435, 247, 2005

Binary stars with magnetic field

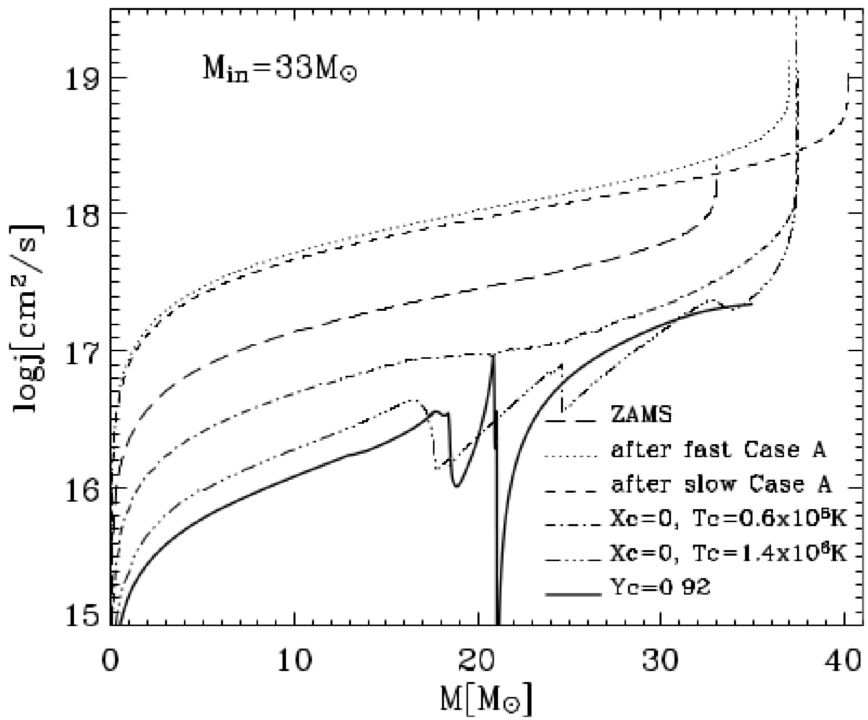

Fig. 20. Specific angular momentum profiles of the secondary star with magnetic fields on the hydrogen ZAMS (long dashed line), after fast (dotted line) and slow (short dashed line) Case A mass transfer, when all hydrogen is exhausted in the center (dot-dashed line), when helium ignites (three dots-dashed line) and and when the central helium abundance is 92% (solid line).

56Ms+33Ms, p=6d

The dynamo model of Spruit (2002) cause a significant angular momentum transport even in the presence of mean molecular weight gradients: magnetic torque keeps star close to solid body rotation

In the magnetic model, the core spin-up due to accretion is stronger than in non-magnetic. It temporarily leads to a core spin rate which is factor of 2...3 above that of a ZAMS star of comparable mass.

Magnetic core-envelope coupling, however, reduces the specific core angular momentum by almost a factor 100 by the time the star has started core helium burning.

At the end of core helium burning and carbon as well, angular momentum of the presupernova core (3 Ms)
Is ~**10^{15}cm^{2}s $^{-1}$** → **no GRB**

Petrovic, Langer, Yoon & Heger A&A, 435, 247, 2005